Effects of valve geometry and tissue anisotropy on the radial stretch and coaptation area of tissue-engineered heart valves

Loerakker, S ; Argento, G ; Oomens, C W J ; Baaijens, F P T

Abstract: Tissue engineering represents a promising technique to overcome the limitations of the current valve replacements, since it allows for creating living autologous heart valves that have the potential to grow and remodel. However, also this approach still faces a number of challenges. One particular problem is regurgitation, caused by cell-mediated tissue retraction or the mismatch in geometrical and material properties between tissue-engineered heart valves (TEHVs) and their native counterparts. The goal of the present study was to assess the influence of valve geometry and tissue anisotropy on the deformation profile and closed configuration of TEHVs. To achieve this aim, a range of finite element models incorporating different valve shapes was developed, and the constitutive behavior of the tissue was modeled using an established computational framework, where the degree of anisotropy was varied between values representative of TEHVs and native valves. The results of this study suggest that valve geometry and tissue anisotropy are both important to maximize the radial strains and thereby the coaptation area. Additionally, the minimum degree of anisotropy that is required to obtain positive radial strains was shown to depend on the valve shape and the pressure to which the valves are exposed. Exposure to pulmonary diastolic pressure only yielded positive radial strains if the anisotropy was comparable to the native situation, whereas considerably less anisotropy was required if the valves were exposed to aortic diastolic pressure.

DOI: https://doi.org/10.1016/j.jbiomech.2013.05.015

Originally published at:
Loerakker, S; Argento, G; Oomens, C W J; Baaijens, F P T (2013). Effects of valve geometry and tissue anisotropy on the radial stretch and coaptation area of tissue-engineered heart valves. Journal of Biomechanics, 46(11):1792-1800.
DOI: https://doi.org/10.1016/j.jbiomech.2013.05.015

Effects of valve geometry and tissue anisotropy on the radial stretch and coaptation area of tissue-engineered heart valves

S. Loerakker, G. Argento, C.W.J. Oomens, F.P.T. Baaijens

Department of Biomedical Engineering
Eindhoven University of Technology
P.O. Box 513, 5600 MB Eindhoven
The Netherlands

Abstract

Tissue engineering represents a promising technique to overcome the limitations of the current valve replacements, since it allows for creating living autologous heart valves that have the potential to grow and remodel. However, also this approach still faces a number of challenges. One particular problem is regurgitation, caused by cell-mediated tissue retraction or the mismatch in geometrical and material properties between tissue-engineered heart valves (TEHVs) and their native counterparts. The goal of the present study was to assess the influence of valve geometry and tissue anisotropy on the deformation profile and closed configuration of TEHVs. To achieve this aim, a range of finite element models incorporating different valve shapes was developed, and the constitutive behavior of the tissue was modeled using an established computational framework, where the degree of anisotropy was varied between values representative of TEHVs and native valves. The results of this study suggest that valve geometry and tissue anisotropy are both important to maximize the radial strains and thereby the coaptation area. Additionally, the minimum degree of anisotropy that is required to obtain positive radial strains was shown to depend on the valve shape and the pressure to which the valves are exposed. Exposure to pulmonary diastolic pressure only yielded positive radial strains if the anisotropy was comparable to the native situation, whereas considerably less anisotropy was required if the valves were exposed to aortic diastolic pressure.

1 Introduction

Heart valve disease remains a major problem worldwide (Takkenberg et al., 2008). Approximately 280.000 heart valve replacements are performed each year (Pibarot and Dumesnil, 2009) and this number still increases (Takkenberg et al., 2008; Dunning et al., 2011). Currently, diseased valves are replaced by either mechanical or bioprosthetic valves. Both types of prostheses significantly enhance the quality of life, but also have several limitations. For example, mechanical valves require lifelong anticoagulation therapy to prevent thromboembolism, and bioprosthetic valves have a limited durability (Kidane et al., 2009; Pibarot and Dumesnil, 2009). Most importantly, both valve substitutes are unable to grow, repair, and remodel in response to changing demands. This represents a major problem for pediatric

patients, who need multiple surgical interventions during their life due to valve deterioration or to accomodate somatic growth (Ackermann et al., 2007; Lee et al., 2011).

Tissue engineering represents a promising technique to overcome the limitations of the current valve replacements, since this approach allows for creating living autologous heart valves that have the potential to grow and remodel. Indeed, previous studies have demonstrated the in vivo functionality of tissue-engineered heart valves (TEHVs) in animal models (Hoerstrup et al., 2000; Flanagan et al., 2009; Gottlieb et al., 2010; Schmidt et al., 2010). However, also this approach faces a number of challenges. For example, mild to severe regurgitation due to retraction of the leaflets has been reported in several studies (Flanagan et al., 2009; Gottlieb et al., 2010), which may even progress with time (Gottlieb et al., 2010). Long-term regurgitation is unacceptable because it will ultimately lead to ventricular failure. Therefore, leaflet retraction is a critical problem that needs to be solved.

TEHVs have different structural properties compared to native valves. This may result in nonphysiological deformation patterns in the tissue when the valve is loaded, and consequently have an influence on both short-term and long-term valve function. In the short term, different deformation patterns in the TEHV can alter the closed configuration of the valve and thereby lead to suboptimal coaptation during diastole. In the long term, as cells remodel the extracellular matrix in response to mechanical stimuli, nonphysiological deformation patterns may lead to altered collagen remodeling compared to native valves. We hypothesize that leaflet retraction leading to regurgitation is, at least partly, caused by this mismatch in structural properties between TEHVs and their native counterparts. Therefore, it may be essential to mimic the deformation profile of native valves in TEHVs to ensure proper valve closure and induce physiological tissue remodeling. In this study, we investigated the influence of the structural properties of TEHVs on the deformation profile and closed configuration of TEHVs.

The geometry of the valve leaflets is one of the factors that influences the deformation profile of TEHVs. The geometry of native valves can be described by the well-known design of Thubrikar (1990), where the load-bearing surfaces of the leaflets are approximated by nearly cylindrical shapes with a curvature in circumferential direction. Using this design, Labrosse et al. (2006) reported that a range of valve dimensions exist for normal aortic heart valves that lead to proper valve function. However, it is not known whether this geometrical range also leads to optimal performance in TEHVs. Moreover, it remains to be questioned whether the Thubrikar design as such provides the ideal shape for TEHVs. In fact, it has been proposed that native leaflets also have a curvature in radial direction (Hamid et al., 1986; Anderson, 2007), which may considerably influence valve performance.

The material properties of TEHVs also affect the mechanical behavior of the valve. Since collagen is the main load-bearing structure in the tissue, particularly the anisotropy of the collagen network is important for its overall function. Native aortic valves exhibit a clear anisotropic material behavior because most collagen fibers are aligned in the circumferential direction (Billiar and Sacks, 2000a; Martin and Sun, 2012). Consequently, extension is limited in this direction, and the tissue will mainly extend in radial direction when the valve is loaded (Billiar and Sacks, 2000a,b; Martin and Sun, 2012). Finite element (FE) models that incorporated this material behavior have also shown that this anisotropic deformation profile affects the stress distribution in the tissue (Li et al., 2001; Luo et al., 2003; Sun et al., 2005), and the opening and closing times during the cardiac cycle (Saleeb et al., 2012). Unfortunately, TEHVs generally have a less distinct collagen anisotropy (Mol et al., 2006), and are therefore exposed to smaller radial strains which can even become negative (Driessen

et al., 2007). This contributes to suboptimal coaptation during the diastolic phase, and maybe also leads to adverse tissue remodeling in the long term. Clearly, this insufficient anisotropy of the collagen network should be improved to enhance the performance of TEHVs. However, it is not clear how much anisotropy is needed to ensure proper valve closure.

In the present study, a computational model that describes the mechanical behavior of cardiovascular tissues (Driessen et al., 2007) was applied to a range of valve shapes to determine the influence of anisotropy on the radial stretch in the valve and the coaptation area for different geometries. In particular, the following questions were addressed: (1) How much anisotropy is needed to prevent negative radial strains? (2) Does the geometry of the TEHV have an influence on this minimum amount of anisotropy? (3) Is this minimum amount of anisotropy different for valves subjected to pulmonary or aortic diastolic pressure?

2 Methods

2.1 Valve geometry

The scaffolds used to culture TEHVs in the host lab have previously been created according to the design of Thubrikar (1990) without any initial coaptation. This geometry is described by five parameters: R_b, R_c, H, H_s, and β (figure 1a). Previously, valves with a diameter of 27 mm were created using the following parameters: $R_b = R_c = 13.5$ mm, $H = 19.15$ mm, $H_s = 3.15$ mm, and $\beta = 0$ °. In the present study, H_s and β were varied to assess the influence of geometrical variations in the Thubrikar design for valves with the same diameter and overall height (see table 1, shapes T1-T9, and figure 1b).

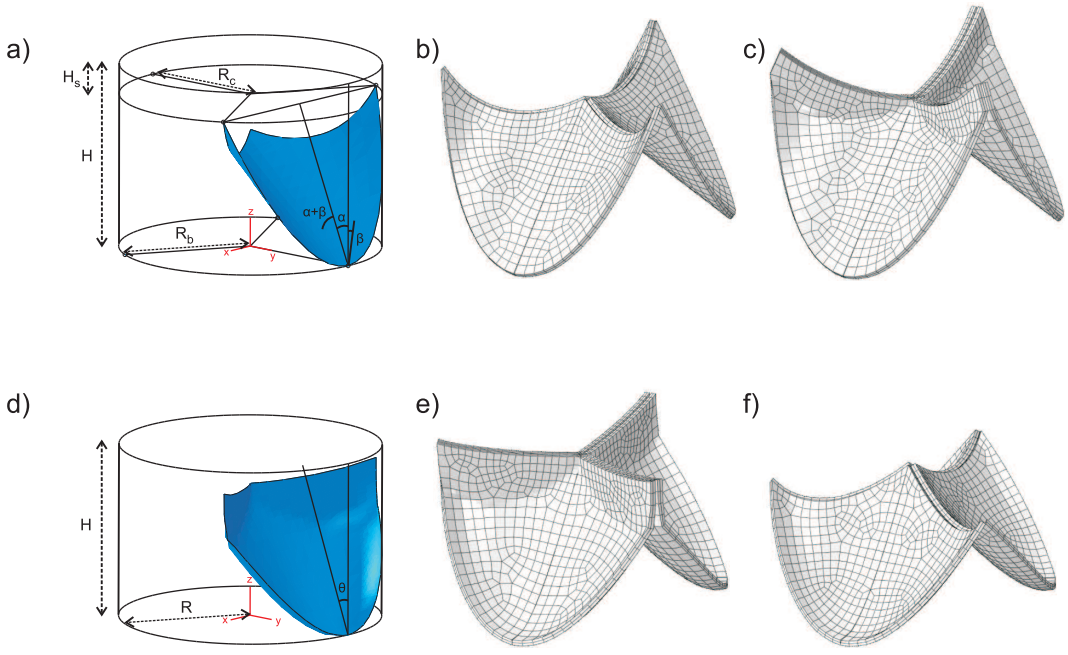

Figure 1: a) Valve leaflet geometry defined by Thubrikar (1990). b) Example of the Thubrikar design without initial coaptation (shape T5, see table 1). c) Example of the Thubrikar design with added initial coaptation (shape T5c). d) Valve leaflet geometry defined by Hamid et al. (1986). e) Example of the Hamid design with initial coaptation (shape H5c). f) Example of the Hamid design where the initial coaptation area has been removed (shape H5).

Table 1: Geometries that were defined using the designs of Thubrikar (1990) and Hamid et al. (1986).

Design Thubrikar (1990)				Design Hamid et al. (1986)			
Shape	H_s [mm]	β [°]	Coaptation	Shape	a [mm]	b [mm]	Coaptation
T1	2.65	0	No	H1	3.1	1.7	No
T2	2.65	2	No	H2	3.1	2.0	No
T3	2.65	4	No	H3	3.1	2.3	No
T4	3.15	0	No	H4	3.4	1.7	No
T5	3.15	2	No	H5	3.4	2.0	No
T6	3.15	4	No	H6	3.4	2.3	No
T7	3.65	0	No	H7	3.7	1.7	No
T8	3.65	2	No	H8	3.7	2.0	No
T9	3.65	4	No	H9	3.7	2.3	No
T1c	2.65	0	Yes	H1c	3.1	1.7	Yes
T2c	2.65	2	Yes	H2c	3.1	2.0	Yes
T3c	2.65	4	Yes	H3c	3.1	2.3	Yes
T4c	3.15	0	Yes	H4c	3.4	1.7	Yes
T5c	3.15	2	Yes	H5c	3.4	2.0	Yes
T6c	3.15	4	Yes	H6c	3.4	2.3	Yes
T7c	3.65	0	Yes	H7c	3.7	1.7	Yes
T8c	3.65	2	Yes	H8c	3.7	2.0	Yes
T9c	3.65	4	Yes	H9c	3.7	2.3	Yes

In addition, the Thubrikar design was compared with the Hamid design, which incorporates the leaflet curvature in both circumferential and radial direction (figure 1d). In this case, the initial leaflet geometry is described by one half of an elliptic paraboloid (Hamid et al., 1986):

$$\frac{x^2}{a^2} + \frac{y^2}{b^2} - z = 0 \tag{1}$$

where parameters a and b determine the curvature in circumferential and radial direction, respectively. This initial geometry was rotated by an angle of $\tan^{-1}(R/(2H))$ (figure 1d), with R the radius of the valve and H the height of the leaflet. Subsequently, points on this surface that cross the planes that separate the leaflet from the other two ($y = \tan(30°)\|x\|$) were mapped onto these planes to obtain the initial coaptation surface (Hamid et al., 1986). Finally, parts of the leaflet where $\sqrt{x^2 + y^2} > R$ were removed. Both the radius and height of the valve were chosen similar to the Thubrikar design ($R = 13.5$ mm, $H = 18$ mm). Parameters a and b were varied to assess the influence of geometrical variations for this design as well (see table 1, shapes H1c-H9c, and figure 1e).

To determine the influence of the initial coaptation surface, valves were created according to the Hamid design where the coaptation surface was removed (see table 1, shapes H1-H9, and figure 1f), as well as according to the Thubrikar design where an initial coaptation surface was added (see table 1, shapes T1c-T9c, and figure 1c).

Each leaflet shape was created with a thickness of 0.5 mm in Abaqus 6.10 (Simulia, Providence, RI). Due to symmetry, only half of the leaflet was modeled and divided into 400-600 elements, depending on the geometry. The main fiber direction in the FE models was assumed to be circumferential, since the known circumferential alignment of the collagen

fibers of native heart valves has also been reported for TEHVs (Cox et al., 2010). For every element, the radial direction was defined as the vector perpendicular to the outer normal of the element $\vec{n}$ and a unit vector in x-direction $\vec{e}_x$: $\vec{v}_2 = (\vec{e}_x \times \vec{n})/\|\vec{e}_x \times \vec{n}\|$. Subsequently, the circumferential direction was calculated as $\vec{v}_1 = \vec{n} \times \vec{v}_2$ (figure 2).

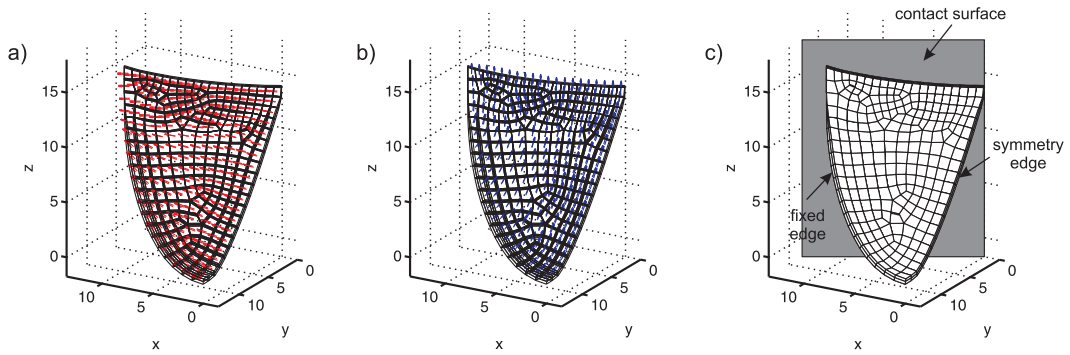

Figure 2: a) Main (circumferential) fiber direction $\vec{v}_1$ in shape H5c. b) Radial direction $\vec{v}_2$ in shape H5c. c) Position of the contact surface and the edges where boundary conditions were applied.

2.2 Material model

The engineered tissue was modeled as a fiber-reinforced material, composed of an anisotropic fiber part (f) with volume fraction ϕ_f and an isotropic matrix part (m) with volume fraction $(1 - \phi_f)$:

$$\boldsymbol{\sigma} = \boldsymbol{\sigma}_m + \boldsymbol{\sigma}_f \tag{2}$$

The isotropic part, describing the contribution of the cells and all extracellular matrix components except collagen, was modeled as a Neo-Hookean material:

$$\boldsymbol{\sigma}_m = (1 - \phi_f)\left(\kappa \frac{\ln(J)}{J}\boldsymbol{I} + \frac{G}{J}(\boldsymbol{B} - J^{2/3}\boldsymbol{I})\right) \tag{3}$$

with $\boldsymbol{F}$ the deformation gradient tensor, $J = \det(\boldsymbol{F})$, $\boldsymbol{B} = \boldsymbol{F} \cdot \boldsymbol{F}^T$, and G and κ the shear and compression modulus, respectively. The anisotropic fiber part, describing the contribution of the collagen network to the total Cauchy stress, was modeled using a discrete number of fiber directions (Driessen et al., 2007):

$$\boldsymbol{\sigma}_f = \sum_{i=1}^{N} \boldsymbol{\tau}_f^i \tag{4}$$

The stress in each fiber direction $\vec{e}_f^{\,i}$ is given by:

$$\boldsymbol{\tau}_f^i = \varphi_f^i \sigma_f^i \vec{e}_f^{\,i} \vec{e}_f^{\,i} \tag{5}$$

where φ_f^i is the fiber volume fraction in each direction, and σ_f^i is the magnitude of the fiber stress depending on the fiber stretch λ_f:

$$\sigma_f = \begin{cases} k_1 \lambda_f^2 \left(e^{k_2(\lambda_f^2 - 1)} - 1\right) & , \lambda_f \geq 1 \\ 0 & , \lambda_f < 1 \end{cases} \qquad \text{where} \qquad \lambda_f = \sqrt{\vec{e}_{f0} \cdot \boldsymbol{F}^T \cdot \boldsymbol{F} \cdot \vec{e}_{f0}} \tag{6}$$

with k_1 and k_2 material parameters, and $\vec{e}_{f0}$ the fiber direction in the undeformed configuration, which was positioned in the plane spanned by vectors $\vec{v}_1$ and $\vec{v}_2$:

$$\vec{e}_{f0} = \cos(\gamma)\vec{v}_1 + \sin(\gamma)\vec{v}_2 \tag{7}$$

where γ is the angle between $\vec{e}_{f0}$ and $\vec{v}_1$. The fiber volume fraction in each direction was described using a Gaussian distribution function:

$$\varphi_f^i = A \exp\left(\frac{-(\gamma-\mu)^2}{2\sigma^2}\right) \qquad \text{with} \qquad A = \frac{\phi_f}{\sum_{i=1}^{N} \exp\left(\frac{-(\gamma-\mu)^2}{2\sigma^2}\right)} \tag{8}$$

where μ is the main fiber angle with respect to $\vec{v}_1$ and σ is the standard deviation of the fiber distribution. The scaling factor A is defined such that the total fiber content equals ϕ_f.

2.3 Material parameters

Similar to Driessen et al. (2007), the total fiber volume fraction ϕ_f was set to 0.5, and the shear modulus of the matrix G was equal to 50 kPa. The isotropic matrix was considered nearly incompressible ($\nu = 0.498$), and the compression modulus κ was equal to $2G(1+\nu)/(3(1-2\nu))$. For the collagen fibers, the parameters for engineered tissue after four weeks culturing with human vena saphena cells were used. The stiffness parameters were equal to $k_1 = 1689$ kPa and $k_2 = 1.93$, the standard deviation of the fiber angle σ was initially set at 63.6 °, and it was assumed that the main fiber orientation was circumferential ($\mu = 0$ °) (Driessen et al., 2007). An angular resolution of 3 ° was used to model the collagen distribution, and the effect of tissue anisotropy was investigated by varying σ between the 63.6 ° and 10.7 °, where the latter standard deviation is comparable to the distribution observed in native valves (Driessen et al., 2007).

2.4 Boundary conditions

Since only one half of the leaflet was used for the FE models, normal displacements at the symmetry edge were suppressed (figure 2c). Furthermore, all the displacements at the lower boundary of the fixed edge were suppressed to simulate the connection of the valve with the stent, and a contact surface ($y = \tan(30°)x$) was added to model the contact between the different leaflets. As all three leaflets were assumed to be similar, the friction coefficient between the leaflet and the contact surface was equal to 0. Finally, a pressure was applied to the top surface to simulate diastolic loading at both pulmonary ($p = 2$ kPa) and aortic ($p = 12$ kPa) conditions.

3 Results

Figure 3 shows the distribution of the stretch in radial direction ($\vec{v}_2$) for a number of valves with different degrees of anisotropy when the valves were subjected to a pressure of 2 kPa. Clearly, a collagen distribution with $\sigma = 63.6°$ resulted in compression of the valve in radial direction ($\lambda_{v2} < 1$) for all geometries, in particular for the valves without an initial coaptation surface (figure 3a,c). A decrease in σ towards native values resulted in an increase in radial stretch for all valves. In the Hamid design with coaptation (figure 3d), extension ($\lambda_{v2} > 1$)

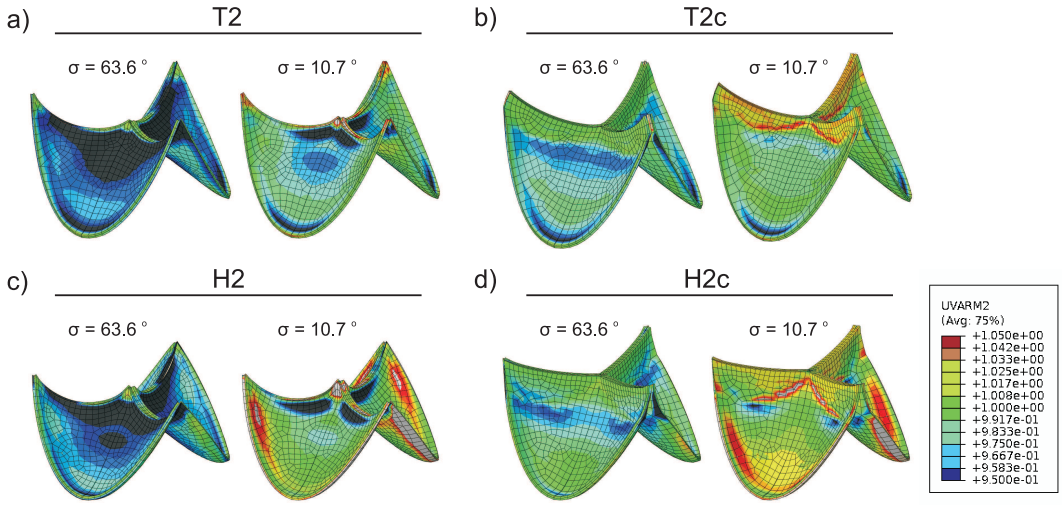

Figure 3: Distribution of the radial stretch in shape T2 (a), T2c (b), H2 (c), and H2c (d) at pulmonary pressure (2 kPa) with different degrees of anisotropy.

of the tissue in radial direction was observed in large parts of the valve, whereas for all other designs the valves were still in compression.

Unfortunately, when the pressure was increased to 12 kPa, several simulations with the Thubrikar and Hamid design without initial coaptation did not converge, particularly the ones incorporating a high degree of anisotropy ($\sigma = 10.7°$). For the simulations that did converge, a decrease in radial stretch was observed (figure 4a,c) for both $\sigma = 63.6°$ and $\sigma = 20°$. For valves with initial coaptation, also compressive stretches were present when $\sigma = 63.6°$ (figure 4b,d). However, an increased level of anisotropy resulted in a clear increase in radial stretch, which was most pronounced for the Hamid design with coaptation (figure 4d). These results, therefore, indicate that the anisotropy of the collagen network has a clear influence on the radial stretches in the valve, and that designs that incorporate an initial coaptation surface lead to higher radial stretches, particularly when the valves are subjected to aortic pressure conditions.

Figure 5 shows the stress-stretch curves in both circumferential and radial direction in the middle of the belly. Results for the Thubrikar design without coaptation at pulmonary pressure show that the circumferential stretch (1.02 – 1.04) was considerably larger than the radial stretch (0.94 – 0.97), and that the stress in radial direction was negative (-2.52 – -1.97 kPa) (figure 5a). Increasing the degree of anisotropy towards native values appeared not to be sufficient to change this pattern. The addition of an initial coaptation surface resulted in positive radial stresses (-0.12 – 4.16 kPa) and a clear increase in radial stretch (0.98 – 0.99), while the circumferential stresses and stretches were hardly affected (1.02 – 1.03). At aortic pressure, the circumferential stretches (1.07 – 1.12) remained larger than the radial stretches (0.88 – 1.04) for the Thubrikar valves with and without coaptation (figure 5b). However, positive radial strains ($\lambda_{v2} > 1$) were present at $\sigma = 10.7°$ if the initial coaptation surface was included. The Hamid design without coaptation showed similar stress-stretch curves at pulmonary pressure as the Thubrikar design when $\sigma = 63.6°$ (final circumferential stretches of 1.01 – 1.03 and radial stretches of 0.95 – 0.98) (figure 5c). However, including a coaptation surface and decreasing σ towards native values was sufficient for this design to obtain positive radial strains ($\lambda_{v2} = 1.01$). At aortic pressure, the radial stretch in this

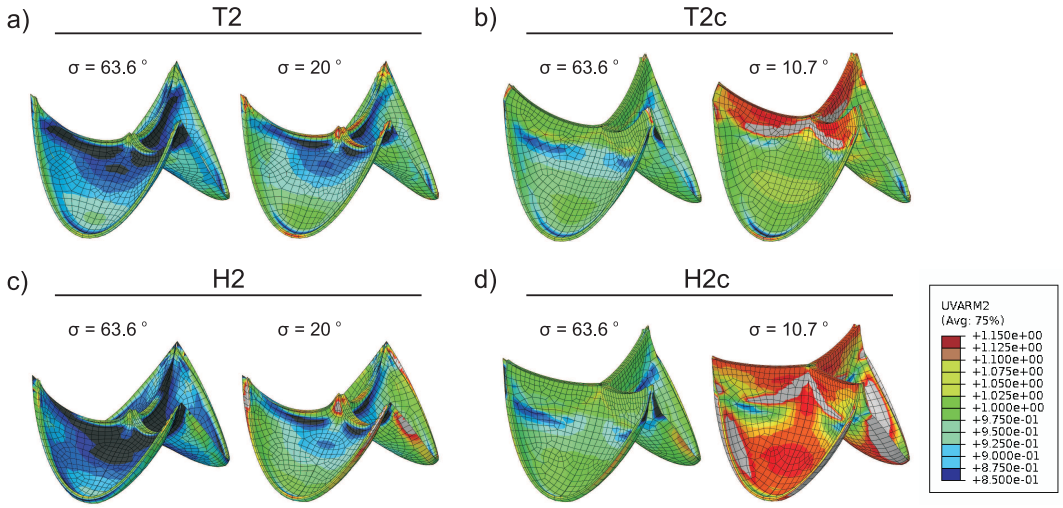

Figure 4: Distribution of the radial stretch in shape T2 (a), T2c (b), H2 (c), and H2c (d) at aortic pressure (12 kPa) with different degrees of anisotropy.

case increased further (1.13) and even exceeded the circumferential stretch (1.06) (figure 5d), which is more representative of the native situation (Billiar and Sacks, 2000a,b; Martin and Sun, 2012).

The final radial stretch in the middle of the belly for all geometries is shown in figure 6. In general, the differences in results when the geometrical parameters of the Thubrikar and Hamid design were varied appeared to be relatively small compared to the differences between the results of the different designs. At pulmonary pressure, positive radial strains could only be obtained with the Hamid design including an initial coaptation surface in 7 out of 9 valves when the anisotropy of the collagen network was comparable to the native situation (with λ_{v2} ranging between 1.00 – 1.01 at $\sigma = 10.7°$) (figure 6d). At aortic pressure, radial stretches were considerably larger with this design, resulting in positive radial strains at $\sigma \leq 30°$ for 6 out of 9 valves (with λ_{v2} ranging between 1.07 – 1.13 at $\sigma = 10.7°$ for all shapes; 1.02 – 1.04 at $\sigma = 20°$ for all shapes; 1.00 – 1.01 at $\sigma = 30°$ for 6 out of 9 shapes) (figure 6h). For the Thubrikar design with initial coaptation, positive radial strains were also present for 7 out of 9 valves at aortic pressure (with λ_{v2} ranging between 1.01 – 1.04), but only if $\sigma = 10.7°$ (figure 6f).

Figure 7 shows the total coaptation area of half the leaflet at pulmonary and aortic pressure for all geometries. Obviously, including an initial coaptation surface resulted in a larger coaptation area compared to the designs without initial coaptation, and the total coaptation area was mainly governed by the size of the initial coaptation surface. Nevertheless, also the degree of anisotropy had a clear effect. Particularly for the Hamid design with initial coaptation, the coaptation area at aortic pressure clearly increased when σ was decreased (37 – 66 mm^2 at $\sigma = 63.6°$ to 49 – 83 mm^2 at $\sigma = 10.7°$) (figure 7h).

4 Discussion

Proper valve closure remains a challenge for heart valve tissue engineering, as regurgitation has been reported in several studies (Flanagan et al., 2009; Gottlieb et al., 2010). Regurgitation is

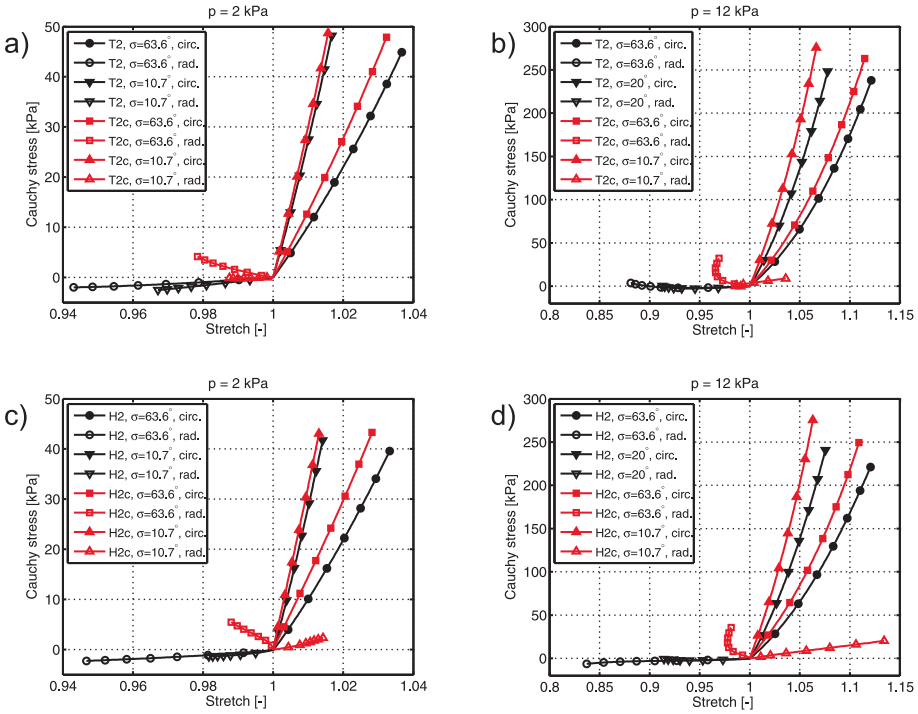

Figure 5: Stress-stretch curves in circumferential and radial direction for a node in the middle of the belly in shapes T2 and T2c at $p = 2$ kPa (a) and 12 kPa (b), and shapes H2 and H2c at $p = 2$ kPa (c) and 12 kPa (d).

mainly caused by cell-mediated retraction of the leaflets (Dijkman et al., 2012; van Vlimmeren et al., 2011, 2012), and to ensure valve closure, these contractile cellular forces should be counteracted by the pressure applied to the valve during diastole. In native valves, the diastolic pressure applied to the valve indeed causes an extension of the tissue in primarily the radial direction (Billiar and Sacks, 2000a,b; Martin and Sun, 2012). In TEHVs, however, the tissue primarily extends in circumferential direction and radial strains can even become negative (Driessen et al., 2007). This difference in deformation profile between TEHVs and native valves is caused by a difference in structural properties, and can thus have a major direct effect on valve closure. In addition, as cells remodel the extracellular matrix in response to mechanical stimuli, these different structural properties of TEHVs can influence tissue remodeling and thereby the ultimate tissue architecture on the long term as well.

In the present study, the importance of valve geometry and tissue anisotropy for the deformation profile and closed configuration of TEHVs was investigated. For this, a range of FE models was created using valve designs proposed by Thubrikar (1990) and Hamid et al. (1986). The constitutive behavior of the tissue was modeled using the computational framework previously developed by Driessen et al. (2007), where the degree of anisotropy of the collagen network was varied between values representative of TEHVs ($\sigma = 63.6°$) and native valves ($\sigma = 10.7°$). The model of Driessen et al. (2007) describes cardiovascular tissues as a mixture of an isotropic part, including cells and all matrix constituents except collagen, and a fibrous part that describes the contribution of the collagen network to the mechanical behavior of the tissue. The collagen network is described as an angular distribution of collagen fibers. In other studies, the tissue has also been approximated as an orthotropic material (Burriesci et al., 1999; Li et al., 2001; Saleeb et al., 2012). However, using a distribution of

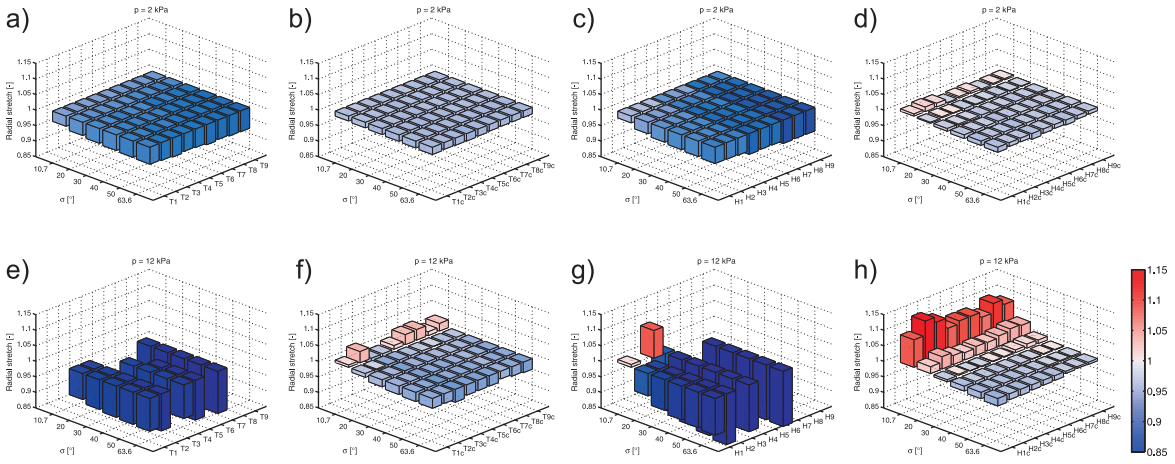

Figure 6: Radial stretch in the middle of the belly at pulmonary (a-d) and aortic (e-h) pressure for the Thubrikar design without initial coaptation (a,e), the Thubrikar design with initial coaptation (b,f), the Hamid design without initial coaptation (c,g), and the Hamid design with initial coaptation (d,h). Unfortunately, several simulations with the Thubrikar and Hamid design without initial coaptation did not converge at 12 kPa, which are indicated by the empty spots.

fiber directions is more realistic as the rotation of fibers and thereby the complex interaction between the circumferential and radial direction is accounted for (Billiar and Sacks, 2000a,b). A limitation of the present study is that the effects of valve geometry and tissue anisotropy were only investigated using a single set of stiffness parameters for the isotropic part and the collagen fibers. Nevertheless, although the results may vary to some extent, the qualitative differences between the different simulations will probably still hold. Therefore, it is unlikely that a different set of parameters would lead to different conclusions in general.

Interestingly, although the radial stretch varied considerably among the different valve shapes and degrees of anisotropy, valve closure was observed in all the FE models with the currrent set of parameters. This is considered to be a shortcoming of the model of Driessen et al. (2007) because the active contribution of the cells is not incorporated. Cells actively pull on and reorganize the extracellular matrix, which results in compaction and retraction of the tissue (Shi and Vesely, 2003; Mol et al., 2005; Neidert and Tranquillo, 2006; Dijkman et al., 2012). Consequently, the initial shapes that are used for creating TEHVs are not the stress-free configurations anymore after four weeks culturing, and separation of the leaflets at the end of the culture period leads to leaflet retraction. The active contribution of the cells and the change in reference configuration were not accounted for in the present study. As a result, closure of the valves (although minimal in some cases) was achieved in all cases. This may not be the case if compaction and retraction are included in the constitutive behavior, as the small radial stretches in some valves may not be sufficient to counteract the cellular traction forces.

The results of this study showed that valve geometry indeed has an influence on the deformation profile and closed configuration of TEHVs. In general, larger radial stretches were obtained with the design of Hamid et al. (1986) than with the design of Thubrikar (1990), and valve shapes incorporating an initial coaptation surface also resulted in larger radial stretches and obviously also larger coaptation areas. The Hamid design mainly differed from the Thubrikar design by having a leaflet curvature in both the circumferential and radial

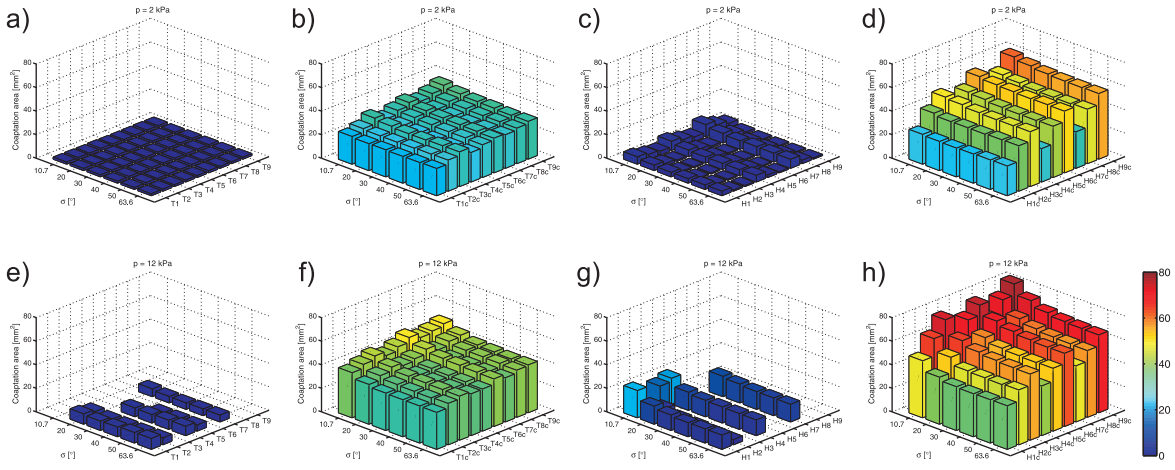

Figure 7: Total coaptation area of half the leaflet at pulmonary (a-d) and aortic (e-h) pressure for the Thubrikar design without initial coaptation (a,e), the Thubrikar design with initial coaptation (b,f), the Hamid design without initial coaptation (c,g), and the Hamid design with initial coaptation (d,h). Unfortunately, several simulations with the Thubrikar and Hamid design without initial coaptation did not converge at 12 kPa, which are indicated by the empty spots.

direction and a larger commissural height. These factors may therefore be important to ensure proper valve function. Nevertheless, the anisotropy of the collagen network appeared to be important as well, as was also suggested in previous studies (Li et al., 2001; Luo et al., 2003; Saleeb et al., 2012). Indeed, an increase in anisotropy resulted in larger radial strains and thereby also larger coaptation areas during loading. Using the properties and degree of anisotropy that were determined for TEHVs after four weeks culturing (Driessen et al., 2007), positive radial strains could not be obtained with any of the valve shapes. At pulmonary pressure, positive strains were only present for the Hamid design with initial coaptation if the anisotropy of the collagen network was comparable to the native situation ($\sigma = 10.7°$). At aortic pressure, the constraints were a little bit less, since the anisotropic behavior of the tissue becomes more pronounced at higher pressures. In this case, positive radial strains could already be obtained at $\sigma = 30°$ if the Hamid design with coaptation was applied.

In summary, the results of the present study suggest that valve geometry and tissue anisotropy are both important factors to increase the radial stretch of TEHVs. Increasing the radial stretch is important because it will improve the closed configuration of the valve and more closely mimics the physiological deformation profile of native valves. Consequently, valves created with scaffolds according to the design of Hamid et al. (1986) may yield better TEHVs than valves created according to the design of Thubrikar (1990). Furthermore, the addition of an initial coaptation surface obviously increases the total coaptation area during loading, and it may also lead to larger radial stretches. In addition, the anisotropy of the tissue appeared to be crucial to increase the radial stretch. Therefore, using an anisotropic scaffold to create TEHVs, which more closely resembles the anisotropic material properties of native valves, can further help to improve the deformation profile and thereby the closed configuration of the valve (Amoroso et al., 2011; Argento et al., 2012), and may also guide the cells to produce a more anisotropic collagen network. Finally, if the tissue is strong enough to withstand the aortic pressure, then exposing TEHVs to this high pressure instead of the lower pulmonary pressure can improve the functionality of TEHVs even further.

Acknowledgments

The authors gratefully acknowledge the funding from the European Union's Seventh Framework Programme ([FP7/2007-2012]) under grant agreement n° 242008.

References

K. Ackermann, G. Balling, A. Eicken, T. Günther, C. Schreiber, and J. Hess. Replacement of the systemic atrioventricular valve with a mechanical prosthesis in children aged less than 6 years: late clinical results of survival and subsequent replacement. *J Thorac Cardiovasc Surg*, 134(3):750–756, 2007.

N.J. Amoroso, A. D'Amore, Y. Hong, W.R. Wagner, and M.S. Sacks. Elastomeric electrospun polyurethane scaffolds: the interrelationship between fabrication conditions, fiber topology, and mechanical properties. *Adv Mater*, 23(1):106–111, 2011.

R.H. Anderson. The surgical anatomy of the aortic root. *MMCTS*, 2007. doi: 10.1510/mmcts.2006.002527.

G. Argento, M. Simonet, C.W.J. Oomens, and F.P.T. Baaijens. Multi-scale mechanical characterization of scaffolds for heart valve tissue engineering. *J Biomech*, 2012. doi: 10.1016/j.jbiomech.2012.07.037.

K.L. Billiar and M.S. Sacks. Biaxial mechanical properties of the natural and gluteraldehyde treated aortic valve cusp - Part I: Experimental results. *J Biomech Eng*, 122(1):23–30, 2000a.

K.L. Billiar and M.S. Sacks. Biaxial mechanical properties of the natural and gluteraldehyde-treated aortic valve cusp - Part II: A structural constitutive model. *J Biomech Eng*, 122 (4):327–335, 2000b.

G. Burriesci, I.C. Howard, and E.A. Patterson. Influence of anisotropy on the mechanical behaviour of bioprosthetic heart valves. *J Med Eng Technol*, 23(6):203–215, 1999.

M.A.J. Cox, J. Kortsmit, N. Driessen, C.V.C. Bouten, and F.P.T. Baaijens. Tissue-engineered heart valves develop native-like collagen fiber architecture. *Tissue Eng Part A*, 16(5):1527–1537, 2010.

P.E. Dijkman, A. Driessen-Mol, L. Frese, S.P. Hoerstrup, and F.P.T. Baaijens. Decellularized homologous tissue-engineered heart valves as off-the-shelf alternatives to xeno- and homografts. *Biomaterials*, 33(18):4545–4554, 2012.

N.J.B. Driessen, A. Mol, C.V.C. Bouten, and F.P.T. Baaijens. Modeling the mechanics of tissue-engineered human heart valve leaflets. *J Biomech*, 40(2):325–334, 2007.

J. Dunning, H. Gao, J. Chambers, N. Moat, G. Murphy, D. Pagano, S. Ray, J. Roxburgh, and B. Bridgewater. Aortic valve surgery: marked increases in volume and significant decreases in mechanical valve use - an analysis of 41,227 patients over 5 years from the Society for Cardiothoracic Surgery in Great Britain and Ireland National Database. *J Thorac Cardiovasc Surg*, 142(4):776–782.e3, 2011.

T.C. Flanagan, J.S. Sachweh, J. Frese, H. Schnöring, N. Gronloh, S. Koch, R.H. Tolba, T. Schmidtz-Rode, and S. Jockenhoevel. In vivo remodeling and structural characterization of fibrin-based tissue-engineered heart valves in the adult sheep. *Tissue Eng Part A*, 15 (10):2965–2976, 2009.

D. Gottlieb, T. Kunal, S. Emani, E. Aikawa, D.W. Brown, A.J. Powell, A. Nedder, G.C. Engelmayr Jr., J.M. Metero-Martin, M.S. Sacks, and J.E. Mayer Jr. In vivo monitoring of function of autologous engineered pulmonary valve. *J Thorac Cardiovasc Surg*, 139(3): 723–731, 2010.

M.S. Hamid, H.N. Sabbah, and P.D. Stein. Influence of stent height upon stresses on the cusps of closed bioprosthetic valves. *J Biomech*, 19(9):759–769, 1986.

S.P. Hoerstrup, R. Sodian, S. Daebritz, J. Wang, E.A. Bacha, D.P. Martin, A.M. Moran, K.J. Guleserian, J.S. Sperling, S. Kaushal, J.P. Vacanti, F.J. Schoen, and J.E. Mayer Jr. Functional living trileaflet heart valves grown in vitro. *Circulation*, 102(19 Suppl 3):1144–1149, 2000.

A.G. Kidane, G. Burriesci, P. Cornejo, S. Sarkar, P. Bonhoeffer, M. Edirisinghe, and A.M. Seifalian. Current developments and future prospects for heart valve replacement therapy. *J Biomed Mater Res B Appl Biomater*, 88(1):290–303, 2009.

M.R. Labrosse, C.J. Beller, F. Robicsek, and M.J. Thubrikar. Geometric modeling of functional trileaflet aortic valves: development and clinical applications. *J Biomech*, 39(14): 2665–2672, 2006.

C. Lee, C.S. Park, C.H. Lee, J.G. Kwak, S.J. Kim, W.S. Shim, J.Y. Song, E.Y. Choi, and S.Y Lee. Durability of bioprosthetic valves in the pulmonary position: long-term follow-up of 181 implants in patients with congenital heart disease. *J Thorac Cardiovasc Surg*, 142 (2):351–358, 2011.

J. Li, X.Y. Luo, and Z.B. Kuang. A nonlinear anisotropic model for porcine aortic heart valves. *J Biomech*, 34(10):1279–1289, 2001.

X.Y. Luo, W.G. Li, and J. Li. Geometrical stress-reducing factors in the anisotropic porcine heart valves. *J Biomech Eng*, 125(5):735–744, 2003.

C. Martin and W. Sun. Biomechanical characterization of aortic valve tissue in humans and common animal models. *J Biomed Mater Res A*, 100(6):1591–1599, 2012.

A. Mol, N.J.B. Driessen, M.C.M. Rutten, S.P. Hoerstrup, C.V.C. Bouten, and F.P.T. Baaijens. Tissue engineering of human heart valve leaflets: a novel bioreactor for a strain-based conditioning approach. *Ann Biomed Eng*, 33(12):1778–1788, 2005.

A. Mol, M.C.M. Rutten, N.J.B. Driessen, C.V.C. Bouten, G. Zünd, F.P.T. Baaijens, and S.P. Hoerstrup. Autologous human tissue-engineered heart valves: prospects for systemic application. *Circulation*, 114(1 Suppl):I152–I158, 2006.

M.R. Neidert and R.T. Tranquillo. Tissue-engineered valves with commissural alignment. *Tissue Eng*, 12(4):891–903, 2006.

P. Pibarot and J.G. Dumesnil. Prosthetic heart valves: selection of the optimal prosthesis and long-term management. *Circulation*, 119(7):1034–1048, 2009.

A.F. Saleeb, A. Kumar, and V.S. Thomas. The important roles of tissue anisotropy and tissue-to-tissue contact on the dynamical behavior of a symmetric tri-leaflet valve during multiple cardiac pressure cycles. *Med Eng Phys*, 2012. doi: 10.1016/j.medengphy.2012.03.006.

D. Schmidt, P.E. Dijkman, A. Driessen-Mol, R. Stenger, C. Mariani, A. Puolakka, M. Rissanen, T. Deichmann, B. Odermatt, B. Weber, M.Y. Emmert, G. Zund, F.P.T. Baaijens, and S.P. Hoerstrup. Minimally-invasive implantation of living tissue-engineered heart valves: a comprehensive approach from autologous vascular cells to stem cells. *J Am Coll Cardiol*, 56(6):510–520, 2010.

Y. Shi and I. Vesely. Fabrication of mitral valve chordae by directed collagen gel shrinkage. *Tissue Eng*, 9(6):1233–1242, 2003.

W. Sun, A. Abad, and M.S. Sacks. Simulated bioprosthetic heart valve deformation under quasi-static loading. *J Biomech Eng*, 127(6):905–914, 2005.

J.J.M. Takkenberg, N.M. Rajamannan, R. Rosenhek, A.S. Kumar, J.R. Carapetis, M.H. Yacoub, and Society for Heart Valve Disease. The need for a global perspective on heart valve disease epidemiology. The SHVD working group on epidemiology of heart valve disease founding statement. *J Heart Valve Dis*, 17(1):135–139, 2008.

M.J. Thubrikar. *The aortic valve*. CRC-Press, 1990.

M.A.A. van Vlimmeren, A. Driessen-Mol, C.W.J. Oomens, and F.P.T. Baaijens. An in vitro model system to quantify stress generation, compaction, and retraction in engineered heart valve tissue. *Tissue Eng Part C Methods*, 17(10):983–991, 2011.

M.A.A. van Vlimmeren, A. Driessen-Mol, C.W.J. Oomens, and F.P.T. Baaijens. Passive and active contributions to generated force and retraction in heart valve tissue engineering. *Biomech Model Mechanobiol*, 11(7):1015–1027, 2012.